Development of droplet microfluidics capable of quantitative estimation of single-cell multiplex proteins

OPEN ACCESS
IOP Publishing
Journal of Micromechanics and Microengineering
J. Micromech. Microeng. **32** (2022) 024002 (8pp)
https://doi.org/10.1088/1361-6439/ac4008

Development of droplet microfluidics capable of quantitative estimation of single-cell multiplex proteins

Hongyu Yang[1,2,4], **Guang Yang**[1,3,4], **Ting Zhang**[1,2], **Deyong Chen**[1,2,3], **Junbo Wang**[1,2,3,*] **and Jian Chen**[1,2,3,*]

[1] State Key Laboratory of Transducer Technology (SKLTT), Aerospace Information Research Institute (AIR) of Chinese Academy of Sciences (CAS), Beijing, People's Republic of China
[2] School of Future Technology (SFT), University of Chinese Academy of Sciences (UCAS), Beijing, People's Republic of China
[3] School of Electronic, Electrical and Communication Engineering (SEECE), University of Chinese Academy of Sciences (UCAS), Beijing, People's Republic of China

E-mail: jbwang@mail.ie.ac.cn and chenjian@mail.ie.ac.cn

Received 23 September 2021, revised 17 November 2021
Accepted for publication 3 December 2021
Published 22 December 2021

Abstract

This study presented constriction microchannel based droplet microfluidics realizing quantitative measurements of multiplex types of single-cell proteins with high throughput. Cell encapsulation with evenly distributed fluorescence labelled antibodies stripped from targeted proteins by proteinase K was injected into the constriction microchannel with the generated fluorescence signals captured and translated into protein numbers leveraging the equivalent detection volume formed by constriction microchannels in both droplet measurements and fluorescence calibration. In order to form the even distribution of fluorescence molecules within each droplet, the stripping effect of proteinase K to decouple binding forces between targeted proteins and fluorescence labelled antibodies was investigated and optimized. Using this microfluidic system, binding sites for beta-actin, alpha-tubulin, and beta-tubulin were measured as $1.15 \pm 0.59 \times 10^6$, $2.49 \pm 1.44 \times 10^5$, and $2.16 \pm 1.01 \times 10^5$ per cell of CAL 27 ($N_{cell} = 15\,486$), $0.98 \pm 0.58 \times 10^6$, $1.76 \pm 1.34 \times 10^5$ and $0.74 \pm 0.74 \times 10^5$ per cell of Hep G2 ($N_{cell} = 18\,266$). Neural net pattern recognition was used to differentiate CAL 27 and Hep G2 cells, producing successful rates of 59.4% (beta-actin), 64.9% (alpha-tubulin), 88.8% (beta-tubulin), and 93.0% in combination, validating the importance of quantifying multiple types of proteins. As a quantitative tool, this approach could provide a new perspective for single-cell proteomic analysis.

Keywords: single-cell analysis, droplet microfluidics, quantitative and multiple measurement, constriction microchannel, proteinase K

(Some figures may appear in colour only in the online journal)

[4] Authors with equal contributions.
[*] Authors to whom any correspondence should be addressed.

1. Introduction

Single-cell proteomic analysis play key roles in the studies with cell-cell variations which mainly includes fields of tumour heterogeneity, immune functions, and stem cell differentiation [1–4].

Optical flow cytometry has functioned as the golden instrument to estimate proteomic expressions of single cells where individual cells bound with antibodies labelled with fluorescence probes flush through a region of capillary under laser excitation and fluorescence detection enabled by photomultiplier tubes [5–8]. Using microbeads with well-defined surface binding sites as calibration, optical flow cytometry is capable of quantitatively estimating single-cell surface proteins [9, 10] while expressions of cytoplasmic and/or nuclear proteins of single cells cannot be quantified because of lacking corresponding microbeads with predefined intracellular binding sites [11]. Recently, mass flow cytometry was developed to measure ∼100 types of proteins of single cells simultaneously by elemental metal isotopes, which still cannot provide numbers of targeted proteins because of lacking calibration approaches [12–14].

Since the feature size of microfluidics (10–100 μm) is comparable with biological cells, a variety of microfluidic platforms including micro-engraving, barcoding microchip and micro flow cytometry were reported for single-cell studies of proteins [15–20]. For large-array microfluidic platforms, single cells were firstly confined within microchambers or microwells, lysed to release targeted proteins which were then captured by pre-coated antibodies for measurements [21, 22]. Although these microfluidics based large arrays could quantitatively estimate single-cell proteins, they could not measure individual cells travelling like a flow cytometry, leading to limited throughputs.

Meanwhile, micro flow cytometry was developed to replace conventional flow cytometry where microfabricated flow channels were leveraged to characterize proteins of individual cells [23]. However, micro flow cytometry could still quantify surface instead of cytosolic proteins without calibrations. Recently, a flow cytometry incorporated with constriction microchannels as calibration structures was developed where fluorescence data of flowing individual cells were processed to protein numbers [24, 25]. However, since the critical dimension of constriction microchannels was ∼10 μm, these microchannels were prone to channel blockage and thus cannot function as a flow cytometry with high working stability.

Aimed to deal with this limitation, this study presented a high-throughput platform of droplet microfluidics capable of quantitative measurements of multiplex proteins of single cells leveraging constriction microchannels as calibration structures. More specifically, cell encapsulation with evenly distributed fluorescence labelled antibodies stripped from targeted proteins by proteinase K was injected into the constriction microchannel. The generated fluorescence signals were captured by multiple photomultiplier tubes and translated into protein numbers leveraging the equivalent detection volume formed by constriction microchannels in both droplet measurements and fluorescence calibration. In comparison to previously developed quantitative approaches where stained single cells were squeezed through constriction microchannels which may lead to channel blockages, cell encapsulation in droplets was adopted in this study, which can deform smoothly through constriction microchannels without the potential concern of channel blockage and thus it can function as a flow cytometry with high throughputs.

2. Methodologies

2.1. Operating schematics

Figure 1 illustrates working principle of this high-throughput droplet microfluidics incorporated with constriction microchannels, which realized quantitative measurements of multiplex proteins of individual cells. This microfluidic platform mainly included a constriction microchannel (cross sectional dimensions lower than a droplet) with a patterned chromium window. As to optical components, a continues-wave solid-state laser was used to provide light for fluorescence excitation and three photomultiplier tubes (PMT) with corresponding filters were adopted to capture fluorescence signals. In addition, individual cells bound with multiple antibodies labelled with fluorescence probes were encapsulated with proteinase K which decoupled the binding forces between target proteins and corresponding antibodies, producing even distributions of fluorescence labelled antibodies within droplets.

In cell measurements, cell encapsulation with evenly distributed fluorescence labelled antibodies was deformed into and occupied the sensitive region (constriction microchannel with metal window) with generated fluorescent pulses captured by multiple photomultiplier tubes. Then, fluorescence pulses were processed into T_r (inclining duration), T_s (steady duration), T_d (declining duration), I_{f1} (fluorescent intensity at wavelength I), I_{f2} (fluorescent intensity at wavelength II), and I_{f3} (fluorescent intensity at wavelength III), where T_r, T_s, and T_d were processed to droplet volume (V_d) leveraging structural parameters of the constriction microchannel as follows:

$$V_d = \frac{\pi}{6} W_c^2 H_c + W_c H_c \left[W_g + \frac{T_s (2W_g + W_c)}{T_r + T_d} \right]. \quad (1)$$

In which W_g stands for metal window's width, W_c and H_c stand for constriction microchannel's width and height.

In fluorescent calibration, solutions made by fluorescence labelled antibodies with a gradient concentration were flushed into the constriction microchannel with corresponding fluorescence intensities measured. Based on the equivalent volume of the detection region in cell measurement and fluorescence calibration, the relationship between fluorescence concentration and intensity was obtained, which was used to translate previously obtained fluorescence intensities of I_{f1}, I_{f2} and I_{f3} into protein concentrations of C_{p1}, C_{p2} and C_{p3} at the single-droplet level. When droplet volumes were taken into consideration, numbers of multiple types of targeted proteins N_{p1}, N_{p2} and N_{p3} of single cells were measured.

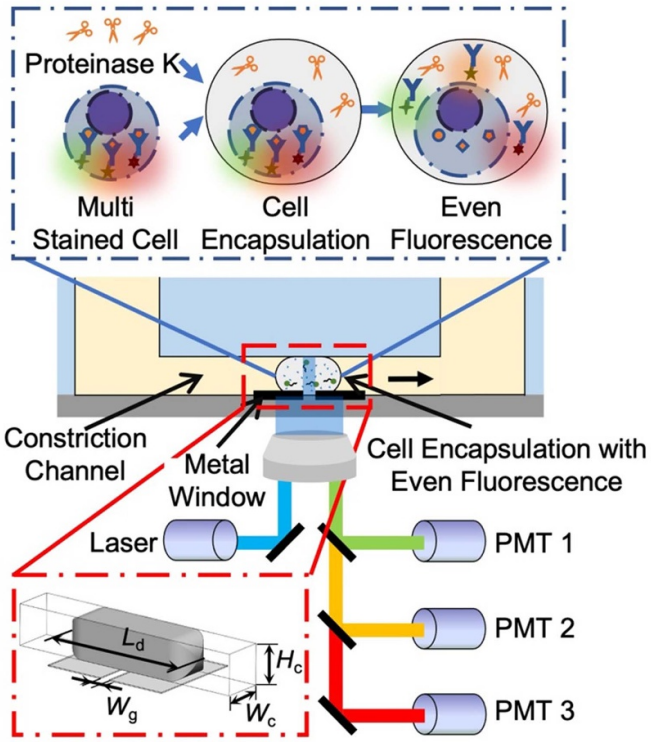

Figure 1. Schematic of high-throughput droplet microfluidics incorporated with constriction microchannels capable of quantitative measurements of multiplex proteins of single cells. Cell encapsulation with evenly distributed fluorescence labelled antibodies stripped from targeted proteins by proteinase K was injected into the constriction microchannel with key geometrical parameters of droplet length of L_d, microchannel width of W_c, microchannel height of H_c, metal window width of W_g. The generated fluorescence signals were captured by multiple photomultiplier tubes and translated into protein numbers leveraging constriction microchannels as the calibration structure.

2.2. Materials

Tumour cell lines used in this study (e.g. CAL 27 and Hep G2) were from National Infrastructure of Cell Line Resources of China (NICLRC). Reagents of culturing biological cells (e.g. Dulbecco's Modified Eagle Medium (DMEM), phosphate buffer saline (PBS), fetal bovine serum and antibiotics) were from Thermo Fisher. Reagents of cell treatment (e.g. paraformaldehyde, triton, and bovine serum albumin) were from Sigma-Aldrich. Antibodies labelled with fluorescent probes included antibodies of beta-actin labelled with Fluorescein isothiocyanate (FITC) (Abcam), antibodies of alpha-tubulin labelled with P-phycoerythrin (PE) and antibodies of beta-tubulin labelled with peridinin-chlorophyll-protein complex (PerCP) (Novus). Proteinase K was purchased from Thermo Fisher as the stripping agent. Note that cytoskeleton proteins (e.g. beta-actin, alpha-tubulin and beta-tubulin) were measured in this study since they were widely used as housekeeping proteins in western blot and flow cytometry.

Materials of device fabrication included negative photoresist of SU-8 (MicroChem), positive photoresist of AZ Electronic, polydimethylsiloxane (PDMS) of SYLGARD 184 (Dow Corning) and aquapel (PPG Industries). Reagents of droplet generation included HFE 7500 supplemented with 008-FluoroSurfactant (Ran Biotechnologies) and iodixanol (OptiPrep™, Sigma-Aldrich).

2.3. Culturing and treatment of cells

A cell incubator (37 °C, 5% CO_2, Forma 3111, Thermo Fisher) was used to culture tumour cell lines of CAL 27 and Hep G2 with DMEM + 10% fetal bovine serum + 1% oi antibiotics. Intracellular staining was conducted with key steps of fixation by 2% paraformaldehyde (15 min @ 4 °C), membrane permeabilization by 0.07% triton (15 min @ 4 °C), blocking by 5% bovine serum albumin (30 min @ 25 °C) and staining by a mixture of antibodies (FITC conjugated antibodies targeting beta-actins, PE conjugated antibodies targeting alpha-tubulins and PerCP conjugated antibodies targeting beta-tubulins) with a 1:100 dilution for 4 h at 37 °C. After staining, cells were resuspended in solutions of 30% iodixanol to match densities. Proteinase K was dissolved in PBS with a group of concentrations for comparison (0.25 mg ml^{-1}, 1 mg ml^{-1} and 5 mg ml^{-1}), which was supplemented with 30% iodixanol to match the density of cell solution.

2.4. Designing and fabricating microfluidic devices

In designing the constriction microchannel based droplet microfluidics, there were three critical geometrical parameters, which were the width of the constriction microchannel (W_c), the height of the constriction microchannel (H_c) and the width of the metal window (W_g). In order to ensure that deformed droplets could effectively fill the sensitive portion of the constriction microchannel, whose cross-section dimensions have to be lower than individual droplets and the width of the metal gap needs to be as small as possible. In this study, by considering limitations of microfabrications, 25 μm height and 20 μm width of the constriction microchannel and 5 μm for the width of the metal window were chosen in this study under the condition of ~50 μm diameter of droplets.

In the fabrication of the constriction microchannel based droplet microfluidics, conventional microfabrication (e.g. hard/soft lithography and PDMS–PDMS bonding) was adopted in this study. In step one, photoresist of SU-8 was spin coated on a glass slide with following patterning enabled by hard lithography to form a mold master of constriction microchannels with a height of 25 μm. In step two, silicone elastomers with 1:15 ratio of curing and base agents was casted to the mold master of SU-8 as soft lithography to transfer the constriction microchannels to the PDMS layer. In step three, the chromium window was made by evaporating a chrome layer of 150 nm in thickness, followed by chromium etching with patterned AZ 1500 photoresist as the mask. Then, a thin PDMS film (~1 μm) was spined on the chromium window to reserve a uniform surface property with the PDMS layer. In step four, PDMS layers with features of constriction microchannels and chromium windows were bonded together after the treatment of oxygen plasma to form enclosed channels.

2.5. Operating devices

In operation, key optical components included a microscope of IX 81 (Olympus), a light source of a laser of OBIS (488 nm, 150 mW, Coherent) and three photomultiplier tubes (H10723-01, H10723-20 and H10722-20, Hamamatsu) coupled with bandpass filters of 534/30 nm, 575/25 nm and 692/40 nm, respectively.

Before detection, the microfluidic device with constriction microchannels was positioned on the microscope for photobleach under the laser power of 35 mW for 30 min. In operation, a pressure of ∼20 kPa from a pressure calibre of Druck PACE-5000 functioned as the driving force to aspirate cell encapsulations with evenly distributed fluorescence labelled antibodies or calibration solutions with gradient concentrations through the constriction microchannel. The laser power for optical detection was set as 5 mW and a data acquisition of USB-6349 at a sample rate of 100 kHz (National Instruments) was used to process the optical data measured by PMT. Note that in experiments of optimizing proteinase K, after the formation of droplets encapsulating stained single cells and proteinase K (0.25 mg ml^{-1}, 1 mg ml^{-1} or 5 mg ml^{-1}), they were incubated for 0 h, 3 h, 6 h, 12 h or 24 h before flushed into constriction microchannels for fluorescent detection.

2.6. Analysing data

The sampled fluorescence signals were firstly processed by a ten-point median filter to get rid of shot noises generated by PMT. Then, pulses representing traveling droplets embedded with stained cells were distinguished by a threshold value which was the basal value without droplets plus ten times of deviations. Note that since empty droplets did not encapsulate fluorescence molecules, they cannot be distinguished from the basal line and thus they were no longer considered in this study.

For individual pulse, it was segmented into an inclining portion, a relatively steady portion and a declining portion leveraging least-square curve fitting of a ladder shape. For the relatively stable domain, under the condition that the peaking level of fluorescence was 1.5 times higher than the mean level of fluorescence, this pulse was regarded as an even encapsulation of antibodies with fluorescence probes. Other pulses were regarded as droplets where fluorescence labelled antibodies still bound with targeted proteins within single cells.

For droplets with evenly distributed fluorescent probes, six key parameters including three time parameters which were T_r, T_s, and T_d, and three intensity parameters which were I_{f1}, I_{f2}, and I_{f3} were obtain by fitting curves. Then, three time parameters were used to calculate droplet volume of V_d following equation (1) in section 2.1 Operating Schematics.

As to data processing in fluorescence calibration, linear curve fitting was firstly conducted for nine groups of preliminary data (e.g. I_{f1} @ 534 nm vs. FITC, I_{f1} @ 534 nm vs. PE, I_{f1} @ 534 nm vs. PerCP, I_{f2} @ 575 nm vs. FITC, I_{f2} @ 575 nm vs. PE, I_{f2} @ 575 nm vs. PE, I_{f3} @ 692 nm vs. FITC, I_{f3} @ 692 nm vs. PE, I_{f3} @ 692 nm vs. PerCP) to form a 3 × 3 compensation matrix made of nine coefficients with normalization. Then three intensity-parameters of I_{f1}, I_{f2}, I_{f3} of a travelling droplet were multiplied with the compensation matrix to form compensated fluorescence intensities at single wavelength, which were I_{f1} @ 534 nm, I_{f2} @ 575 nm and I_{f3} @ 692 nm. Based on coefficients of I_{f1} @ 534 nm vs. FITC, I_{f2} @ 575 nm vs. PE and I_{f3} @ 692 nm vs. PerCP, these fluorescence intensities were translated into concentrations of the three detection targets (C_{p1}, C_{p2}, C_{p3}). The final results of the numbers of detected proteins (N_{p1}, N_{p2}, N_{p3}) were obtained by combining the intermediate results of droplet volumes of V_d and protein concentrations of C_{p1}, C_{p2}, C_{p3}.

2.7. Statistics

All the experiments were conducted at least with three groups. Additionally, Neural Net Pattern Recognition App was used to conduct cell-type classification (MATLAB 2018b, MathWorks). For the classifications of CAL 27 and Hep G2, expressions of beta-actins, alpha-tubulins and beta-tubulins at the single-cell level were used as single or combined inputting datasets, which were then divided into 70% for training, 15% for validation, and 15% for testing. The classification result was represented by a confusion matrix, in which the value at the lower right corner represented the proportion of correctly classified samples to the total samples, which was termed as 'successful rate'. More specifically, 50% of the successful rate indicated that two samples were identical while a successful rate of 100% suggested that two samples were 100% different.

3. Results

Droplet microfluidics has gained a lot of attentions recently since it leverages two immiscible liquids to form large amounts of monodisperse tiny rooms, which are especially suitable for single-cell analysis [26–28]. As to droplet based single-cell proteomic analysis, the majority of previous studies focused on the measurements of secreted proteins which were bound with co-encapsulated microbeads within droplets [29–32]. As to the measurements of membrane or intracellular proteins of single cells, droplet microfluidics has functioned as a qualitative rather than quantitative tool because of lacking calibration methods of translating fluorescence signals into numbers of single-cell proteins [11, 33].

Most recently, a droplet platform was reported to realize quantitative estimation of single-cell proteins leveraging constriction microchannels as calibration structures, which, however, cannot work properly under the condition of uneven distributions of fluorescence within droplets and also can only measure single rather than multiplex proteins [34]. In order to deal with this problem, in this study, proteinase K was incorporated with stained individual cells to form evenly distributions of fluorescence within droplets, which were forced to travel through constriction microchannels with multiplex types of single-cell proteins quantified leveraging multiple photomultiplier tubes with fluorescence crosstalk compensated.

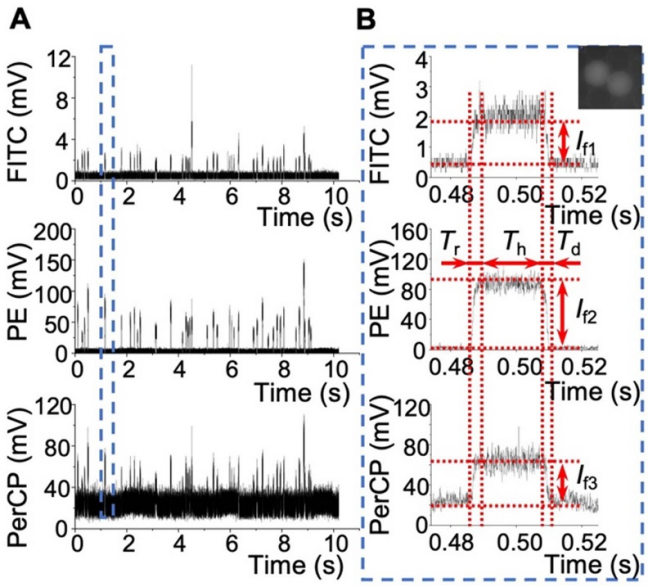

Figure 2. (A) Raw intensities of fluorescence for droplets embedded with individual CAL 27 cells bound with anti-beta-actin antibody labelled with the fluorescent probe of FITC, anti-alpha-tubulin antibody labelled with the fluorescent probe of PE, and anti-beta-tubulin antibody labelled with the fluorescent probe of PerCP. (B) For individual droplet, three fluorescence pulses with ladder shapes were captured and then key markers of I_{f1}, I_{f2}, I_{f3}, T_r, T_s, and T_d were located using ladder-shape fitting.

Figure 2(a) shows preliminary intensities of fluorescence for droplets embedded with individual CAL 27 cells which travelled through the constriction microchannel. For each droplet with embedded single cells, three pulses with wavelengths of 534 nm of FITC for beta-actins, 575 nm of PE for alpha-tubulins and 692 nm of PerCP for beta-tubulins were measured. By fitting with ladder pulses, six markers of T_r, T_s, T_d, I_{f1}, I_{f2}, and I_{f3} were collected (see figure 2(b)).

Based on the results of measuring droplets encasulating individual CAL 27 cells, T_r, T_s, and T_d were quantified as 1.17 ± 0.35, 26.89 ± 7.68 and 1.16 ± 0.58 ms. Thus, the processing speed of this microfluidic approach was estimated as 10–100 cells per sec since the time durations of individual pulses were ~10 ms. In addition, I_{f1}, I_{f2}, and I_{f3} were quantified as 1.80 ± 0.76 mV, 62.87 ± 37.62 mV and 27.71 ± 3.66 mV. Note that since these three parameters were determined by fluorescence intensities of FITC @ 534 nm, PE @ 575 nm and PerCP @ 692 nm respectively, these values of I_{f1}, I_{f2}, and I_{f3} cannot be effectively compared, which need to be translated into protein concentrations within droplets and protein numbers of individual cells.

In this constriction microchannel based droplet microfluidics, fluorescence labelled antibodies should be effectively stripped from individual cells to form an even distribution of fluorescence molecules within each droplet. This was full of challenges since the most effective stripping agents were based on surfactants (e.g. sodium dodecyl sulfate (SDS)) which significantly decrease the stability of droplets. As to conventional strippers used in western blotting, they were formulated with the addition of strong acids or bases, which not only compromised the stability of droplets but also had side effects on the performance of fluorescence probes.

In order to address this issue, proteinase K from a family of endolytic proteases was adopted in this study and its effect on stripping fluorescence labelled antibodies within droplets was investigated. Figure 3 shows percentages of encapsulating CAL 27 cells with fully stripped antibodies and thus evenly distributed fluorescence under a variety of incubation time and concentrations of proteinase K. Based on this figure, it was observed that with increases in concentrations of proteinase K and incubation durations, percentages of cell encapsulation with even fluorescence distributions were increased accordingly and under the condition of 1 mg ml^{-1} proteinase K and an incubation duration of 6 h, 100% cell encapsulation demonstrated even fluorescence distributions for all the three types of proteins. These results validated the functionality of proteinase K in stripping fluorescence labelled antibodies from targeted proteins within cells and thus 1 mg ml^{-1} proteinase K with an incubation duration of 6 h was included in further experiments to characterize multiple protein expressions for both CAL 27 and Hep G2 cells. Note that for Hep G2 cells, 1 mg ml^{-1} proteinase K with an incubation duration of 6 h was directly used without optimization, which was observed to also produce 100% droplets with evenly distributed fluorescence.

In the measurements of multiple types of single-cell proteins, fluorescence calibration was a key component. Figure 4 illustrates calibration results of fluorescence intensity at 534 nm vs. concentration of anti-beta-actin antibody labelled with fluorescent probes of FITC, fluorescence intensity at 575 nm vs. concentration of anti-alpha-tubulin antibody labelled with PE, and fluorescence intensity at 692 nm vs. concentration of anti-beta-tubulin antibody labelled with PerCP. These results indicated that linear correlations were found between fluorescence intensities and fluorescence antibodies, which were $I_{f1} = 0.09 \times C_{FITC} + 0.27$ at 534 nm, $I_{f2} = 16.59 \times C_{PE} + 1.63$ at 575 nm and $I_{f3} = 2.99 \times C_{PerCP} + 18.12$ at 692 nm. Note that the intercepts of the curves represented the offset voltages of the photomultipliers, which were the mean values of the basal fluorescence intensities in the absence of droplets.

Based on aforementioned calibration curves, preliminary fluorescence intensities (e.g. I_{f1}, I_{f2} and I_{f3}) were processed into single-droplet concentrations of anti-beta-actin antibodies labelled with the fluorescent probe of FITC, anti-alpha-tubulin antibodies labelled with the fluorescent probe of PE, anti-beta-tubulin antibodies labelled with the fluorescent probe of PerCP, which were 16.96 ± 8.47 nM, 3.76 ± 2.31 nM and 3.13 ± 1.27 nM for CAL 27 cells and 17.59 ± 10.82 nM, 3.22 ± 2.66 nM and 1.28 ± 0.77 nM for Hep G2 cells, respectively (see figure 5). In addition, based on equation (1), time parameters (e.g. T_r, T_s, and T_d) were processed into droplet volumes of 116.8 ± 33.2 pL for CAL 27 cells and 96.8 ± 28.7 pL for Hep G2 cells. Based on these results, it was observed that for both CAL 27 cells and Hep G2 cells, the expressions of beta-actins were much higher than

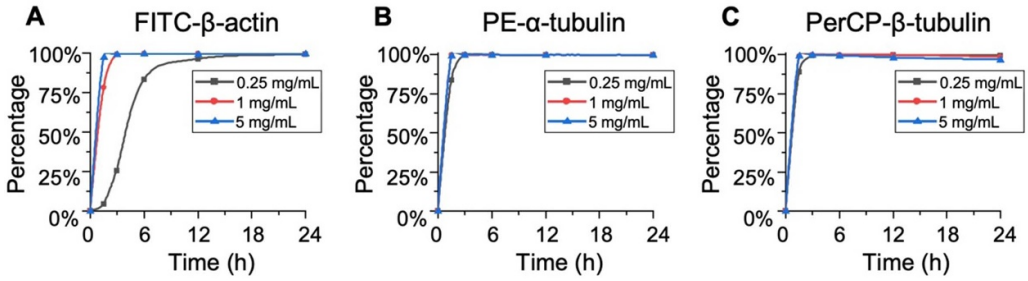

Figure 3. Percentage of droplets encapsulating individual CAL 27 cells with evenly distributed fluorescence labelled antibodies ((A) FITC-beta-actin, (B) PE-alpha-tubulin, and (C) PerCP-beta-tubulin) under a variety of incubation time and concentration of proteinase K, which functioned as the stripper to decouple the binding forces between targeted proteins and corresponding fluorescence labelled antibodies.

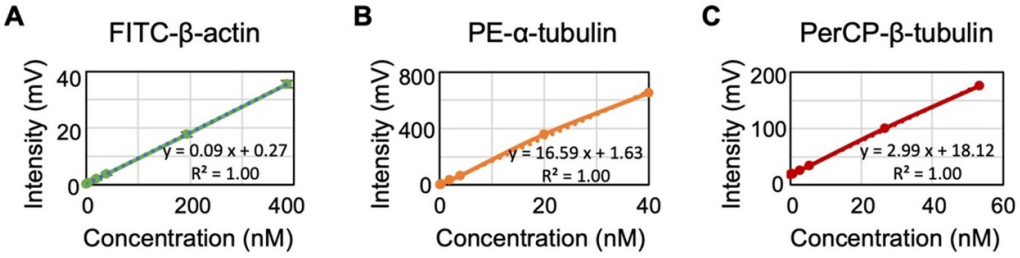

Figure 4. Liner calibration curves of (A) fluorescence intensity at 534 nm vs. concentration of anti-beta-actin antibody labelled with the fluorescent probe of FITC, (B) fluorescence intensity at 575 nm vs. concentration of anti-alpha-tubulin antibody labelled with the fluorescent probe of PE, and (C) fluorescence intensity at 692 nm vs. concentration of anti-beta-tubulin antibody labelled with the fluorescent probe of PerCP.

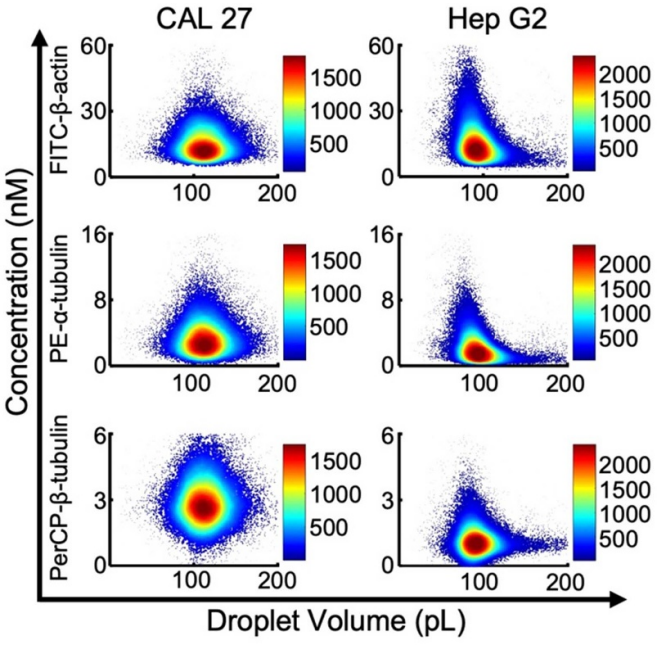

Figure 5. 2D scatter plots of concentrations of beta-actin labelled with FITC, alpha-tubulin labelled with PE and beta-tubulin labelled with PerCP vs. droplet volume for individual CAL 27 and Hep G2 cells.

alpha-tubulins and beta-tubulins of single cells. While the expressions of alpha-tubulins and beta-tubulins were compared, CAL 27 cells demonstrated comparable values while in Hep G2 cells, the expressions of alpha-tubulins were as twice as beta-tubulins.

When the calculated protein concentrations and droplet volumes were combined together, the numbers of single-cell binding sites (N_p) for beta-actin, alpha-tubulin, and beta-tubulin were measured as $1.15 \pm 0.59 \times 10^6$, $2.49 \pm 1.44 \times 10^5$, and $2.16 \pm 1.01 \times 10^5$ per cell of CAL 27 ($N_{cell} = 15\,486$), $0.98 \pm 0.58 \times 10^6$, $1.76 \pm 1.34 \times 10^5$ and $0.74 \pm 0.74 \times 10^5$ per cell of Hep G2 ($N_{cell} = 18\,266$) (see figure 6(a)). In comparison to previously reported values, N_p reported in this study fell in the same ranges (e.g. $0.6–1.5 \times 10^6$ per cell of beta-actin, $0.6–3.0 \times 10^5$ per cell of alpha-tubulin and $0.6–3.0 \times 10^5$ per cell of beta-tubulin [25, 34]), which to an extent validated the performance of the droplet platform reported here.

Figure 6(b) shows confusion matrixes based on neural net pattern recognition to differentiate CAL 27 vs. Hep G2 cells under single parameters of beta-actin, alpha-tubulin and beta-tubulin only or three parameters in combination. When single parameters were used for the cell-type classification, limited successful rates were found, which were 59.4% based on beta-actin only, 64.9% based on alpha-tubulin only and 88.8% based on beta-tubulin only. When these three parameters were used in combination, the successful rate of differentiating CAL 27 from Hep G2 was increased to 93.0%. These results confirmed the importance of quantifying multiple types of proteins which can prove a more comprehensive evaluation of single cells in comparison to results using one protein type.

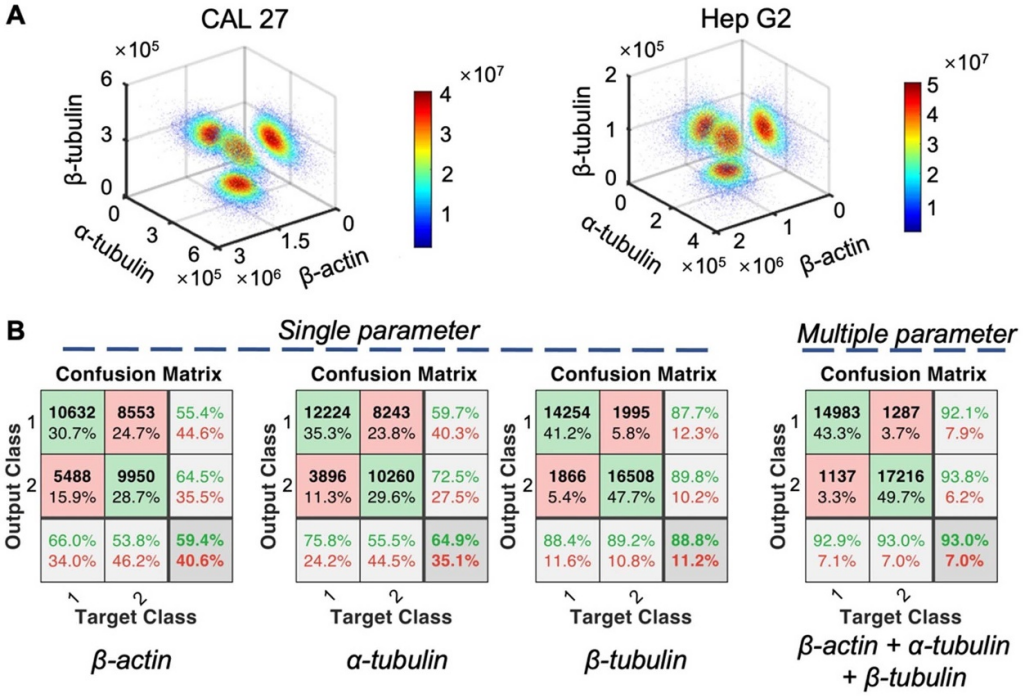

Figure 6. (A) 3D scatter plots of the three types of proteins (beta-actin, alpha-tubulin and beta-tubulin) of individual CAL 27 (n_{cell} = 15 486) and Hep G2 (n_{cell} = 18 266) cells. (B) Confusion matrixes to differentiate CAL 27 vs. Hep G2 cells under single parameters of beta-actin, alpha-tubulin and beta-tubulin only or three parameters in combination where the values in the bottom right corner indicated successful rates of classifying CAL 27 and Hep G2.

Data availability statement

All data that support the findings of this study are included within the article (and any supplementary files).

Acknowledgments

Authors thank National Natural Science Foundation of China of NSFC with Grant Numbers of 61825107, 61922079 and 62001042, Youth Innovation Promotion Association (Y201927), Instrument Research and Development (GJJSTD20210004), and Key Project (QYZDB-SSW-JSC011) of Chinese Academy of Sciences (CAS).

ORCID iD

Jian Chen https://orcid.org/0000-0003-4612-3279

References

[1] Savage N 2015 Proteomics: high-protein research *Nature* **527** S6–7
[2] Doerr A 2019 Single-cell proteomics *Nat. Methods* **16** 20
[3] Labib M and Kelley S O 2020 Single-cell analysis targeting the proteome *Nat. Rev. Chem.* **4** 143–58
[4] Liu L, Chen D, Wang J and Chen J 2020 Advances of single-cell protein analysis *Cells* **9** 1271
[5] Telford W G, Hawley T, Subach F, Verkhusha V and Hawley R G 2012 Flow cytometry of fluorescent proteins *Methods* **57** 318–30
[6] Chattopadhyay P K and Roederer M 2012 Cytometry: today's technology and tomorrow's horizons *Methods* **57** 251–8
[7] Adan A, Alizada G, Kiraz Y, Baran Y and Nalbant A 2017 Flow cytometry: basic principles and applications *Crit. Rev. Biotechnol.* **37** 163–76
[8] Binek A, Rojo D, Godzien J, Rupérez F J, Nuñez V, Jorge I, Ricote M, Vázquez J and Barbas C 2019 Flow cytometry has a significant impact on the cellular metabolome *J. Proteome Res.* **18** 169–81
[9] Maher K J and Fletcher M A 2005 Quantitative flow cytometry in the clinical laboratory *Clin. Appl. Immunol. Rev.* **5** 353–72
[10] Hoffman R A, Wang L, Bigos M and Nolan J P 2012 NIST/ISAC standardization study: variability in assignment of intensity values to fluorescence standard beads and in cross calibration of standard beads to hard dyed beads *Cytometry* A **81** 785–96
[11] Fan B, Li X, Chen D, Peng H, Wang J and Chen J 2016 Development of microfluidic systems enabling high-throughput single-cell protein characterization *Sensors* **16** 232
[12] Bendall S C *et al* 2011 Single-cell mass cytometry of differential immune and drug responses across a human hematopoietic continuum *Science* **332** 687–96
[13] Di Palma S and Bodenmiller B 2015 Unraveling cell populations in tumors by single-cell mass cytometry *Curr. Opin. Biotechnol.* **31** 122–9
[14] Spitzer M H and Nolan G P 2016 Mass cytometry: single cells, many features *Cell* **165** 780–91
[15] Whitesides G M 2006 The origins and the future of microfluidics *Nature* **442** 368–73
[16] Chen P, Chen D, Li S, Ou X and Liu B-F 2019 Microfluidics towards single cell resolution protein analysis *TrAC—Trends Anal. Chem.* **117** 2–12

[17] Lecault V, White A K, Singhal A and Hansen C L 2012 Microfluidic single cell analysis: from promise to practice *Curr. Opin. Chem. Biol.* **16** 381–90
[18] Fung C W, Chan S N and Wu A R 2020 Microfluidic single-cell analysis-toward integration and total on-chip analysis *Biomicrofluidics* **14** 021502
[19] Fu A Y, Spence C, Scherer A, Arnold F H and Quake S R 1999 A microfabricated fluorescence-activated cell sorter *Nat. Biotechnol.* **17** 1109–11
[20] Wu M, Perroud T D, Srivastava N, Branda C S, Sale K L, Carson B D, Patel K D, Branda S S and Singh A K 2012 Microfluidically-unified cell culture, sample preparation, imaging and flow cytometry for measurement of cell signaling pathways with single cell resolution *Lab Chip* **12** 2823–31
[21] Love J C, Ronan J L, Grotenbreg G M, van der Veen A G and Ploegh H L 2006 A microengraving method for rapid selection of single cells producing antigen-specific antibodies *Nat. Biotechnol.* **24** 703–7
[22] Fan R *et al* 2008 Integrated barcode chips for rapid, multiplexed analysis of proteins in microliter quantities of blood *Nat. Biotechnol.* **26** 1373–8
[23] Li X, Fan B, Cao S, Chen D, Zhao X, Men D, Yue W, Wang J and Chen J 2017 A microfluidic flow cytometer enabling absolute quantification of single-cell intracellular proteins *Lab Chip* **17** 3129–37
[24] Li X, Fan B, Liu L, Chen D, Cao S, Men D, Wang J and Chen J 2018 A microfluidic fluorescent flow cytometry capable of quantifying cell sizes and numbers of specific cytosolic proteins *Sci. Rep.* **8** 14229
[25] Liu L *et al* 2020 Development of microfluidic platform capable of high-throughput absolute quantification of single-cell multiple intracellular proteins from tumor cell lines and patient tumor samples *Biosens. Bioelectron.* **155** 112097
[26] Kang D-K, Monsur Ali M, Zhang K, Pone E J and Zhao W 2014 Droplet microfluidics for single-molecule and single-cell analysis in cancer research, diagnosis and therapy *TrAC—Trends Anal. Chem.* **58** 145–53
[27] Wen N, Zhao Z, Fan B, Chen D, Men D, Wang J and Chen J 2016 Development of droplet microfluidics enabling high-throughput single-cell analysis *Molecules* **21** 881
[28] Matula K, Rivello F and Huck W T S 2020 Single-cell analysis using droplet microfluidics *Adv. Biosyst.* **4** e1900188
[29] Konry T, Dominguez-Villar M, Baecher-Allan C, Hafler D A and Yarmush M L 2011 Droplet-based microfluidic platforms for single T cell secretion analysis of IL-10 cytokine *Biosens. Bioelectron.* **26** 2707–10
[30] Chokkalingam V, Tel J, Wimmers F, Liu X, Semenov S, Thiele J, Figdor C G and Huck W T S 2013 Probing cellular heterogeneity in cytokine-secreting immune cells using droplet-based microfluidics *Lab Chip* **13** 4740–4
[31] Eyer K *et al* 2017 Single-cell deep phenotyping of IgG-secreting cells for high-resolution immune monitoring *Nat. Biotechnol.* **35** 977–82
[32] Ding R *et al* 2020 Rapid isolation of antigen-specific B-cells using droplet microfluidics *RSC Adv.* **10** 27006–13
[33] Shembekar N, Hu H X, Eustace D and Merten C A 2018 Single-cell droplet microfluidic screening for antibodies specifically binding to target cells *Cell Rep.* **22** 2206–15
[34] Yang H Y, Wei Y, Fan B, Liu L, Zhang T, Chen D, Wang J and Chen J 2021 A droplet-based microfluidic flow cytometry enabling absolute quantification of single-cell proteins leveraging constriction channel *Microfluid. Nanofluid.* **25** 11